# Cdc25A-inhibitory properties and antineoplastic activity of bisperoxovanadium analogues

**P. James Scrivens,[1,2] Moulay A. Alaoui-Jamali,[1,2,3,4,5] Giuseppe Giannini,[1] Taiqi Wang,[1,5] Martin Loignon,[1] Gerald Batist,[1,2,3,4,5] and Victor A. Sandor[1,5]**

**[1] Lady Davis Institute for Medical Research, SMBD Jewish General Hospital, Montreal, Quebec, Canada; [2] Division of Experimental Medicine, Department of Medicine, [3] Department of Pharmacology and Therapeutics, [4] Departments of Medicine and Oncology, McGill University, Montreal, Quebec, Canada; and [5] Montreal Centre for Experimental Therapeutics in Cancer, Montreal, Quebec, Canada**

## Abstract

**Bisperoxovanadium (bpV) compounds are irreversible protein tyrosine phosphatase (PTP) inhibitors with a spectrum of activity distinct from that of vanadium salts. We studied the efficacy of a panel of bpVs as antineoplastic agents *in vitro* and *in vivo* with a view to investigating phosphatases as potential antineoplastic targets. The Cdc25A dual-specificity phosphatase is an oncoprotein required for progression through $G_1$-S. It cooperates with oncogenic Ras to transform cells and is overexpressed in several cancers. Cdc25A is therefore an attractive candidate phosphatase target for the antineoplastic activity of bpV compounds. Cytotoxicity was examined in 28 cancer cell lines and *in vivo* efficacy was examined in a DA3 murine mammary carcinoma model. *In vitro* phosphatase assays were used to directly measure phosphatase inhibition, comparing Cdc25A to hVH2/DSP4, leukocyte antigen related/receptor type PTPF catalytic domain (LAR), *Yersinia pestis* phosphatase (YOPH), and T-cell PTPase/non-receptor type PTP2 (TCPTP). CDK2 activity and Rb phosphorylation were examined by immunocomplex kinase assays and Western blot. Cdc25A is at least 20-fold more sensitive to bpV inhibition than hVH2/DSP4, and 3- to 10- fold more sensitive than TCPTP and LAR. bpV inhibition of Cdc25A in cells leads to CDK2 inactivation and hypophosphorylation Rb, resulting in $G_1$-S arrest and induction of p53-independent apoptosis. The most cytotoxic analogue, bpV[4,7-dimethyl-1,10-phenanthroline-bisperoxo-oxo-vanadium (Me2Phen)], shows submicromolar $IC_{50}$s against a panel of cell lines and inhibited tumor growth by 80% in mice. These results demonstrate that bpVs may have significant antineoplastic activity. In addition, they are *in vitro* and *in vivo* inhibitors of phosphatases including Cdc25A, suggesting that phosphatases may be appropriate targets for novel antineoplastic agents and that further development of these agents, targeting them to specific phosphatases such as CDC25A, may lead to novel agents with enhanced antineoplastic activity. (Mol Cancer Ther. 2003;2:1053–1059)**

## Introduction

Vanadium salts are non-specific protein tyrosine phosphatase (PTP) and dual-specificity phosphatase inhibitors, with the highly coordinated metal core mimicking phosphate (1). Vanadate and pervanadate have been tested for antineoplastic activity, with mixed results (2, 3). Clearly, although they are potent phosphatase inhibitors, the lack of specificity of simple vanadium compounds makes them unsuitable for pharmacological applications.

In contrast, several groups have reported the synthesis and purification of discrete peroxo- and bisperoxovanadium (bpV) compounds and their application as experimental therapeutics in the treatment of diabetes (4–6), where PTP inhibition results in insulin mimesis through sustained activation of the insulin receptor kinase (7). These compounds take advantage of the high coordination potential of vanadium to multiply ligate the metal core, allowing for the creation of a wide variety of stable compounds with increased substrate specificity. Furthermore, the inhibition of PTPs by these compounds is believed to be irreversible (7), resulting from oxidation of the catalytic cysteine.

The Cdc25A dual-specificity phosphatase is a central player in the cell cycle and is highly regulated by DNA damage checkpoints. It is referred to as ''dual-specificity'' in that it falls into a small group of phosphatases that act on both phosphotyrosine and phosphothreonine/serine residues. Cdc25 isoforms activate Cdks by removing inhibitory phosphates from adjacent threonine and tyrosine (T14/Y15) residues. Unlike other $G_1$-S checkpoint mediators such as p53 and Rb, Cdc25A is a proto-oncoprotein, not a tumor suppressor. It is overexpressed in several cancers (8, 9) and can cooperate with oncogenic

Received 12/2/02; revised 3/25/03; accepted 7/22/03.

The costs of publication of this article were defrayed in part by the payment of page charges. This article must therefore be hereby marked advertisement in accordance with 18 U.S.C. Section 1734 solely to indicate this fact.

**Note:** The content of this article does not necessarily reflect the position or the policy of the Government of the United States, and no official endorsement should be inferred. Research was conducted in compliance with the Animal Welfare Act Regulations and other Federal statutes relating to animals and experiments involving animals and adheres to the principles set forth in the Guide for Care and Use of Laboratory Animals, National Research Council, 1996.

**Grant support:** Canadian Institutes of Health Research and the Canadian Breast Cancer Research Initiative. P.J.S. is the recipient of a BCRP Predoctoral Fellowship #DAMD17-02-1-0478 sponsored by the Department of the Army. The U.S. Army Medical Research Acquisition Activity 820 Chandler Street, Fort Detrick, MD 21702-5014 is the awarding and administering acquisition office.

**Requests for Reprints:** Moulay A. Alaoui-Jamali, Lady Davis Institute for Medical Research, Room 523, Jewish General Hospital, 3755 chemin cote Ste Catherine, Montreal, P.Q., H3T 1E2 Canada.
Phone: (514) 340-8222 ext. 3438; Fax: (514) 340-7576.
E-mail: malaou@po-box.mcgill.ca

Ras to transform rodent fibroblasts (10). It is one of a limited number of ''activating phosphatases,'' the activity of which serves to promote cell cycle progression and/or signaling cascades. Pharmacological inhibition of Cdc25A is therefore predicted to have great antineoplastic potential. Cdc25 family members have recently been defined as primary mediators of several major DNA damage checkpoints, being phosphorylated and inactivated by Chk1, Chk2, and p38 kinases in response to UV, ionizing radiation (IR), and other genotoxic stresses (11–13). The Cdc25 family of phosphatases represents an enticing target not only because of its central role in the cell cycle, but because of its unique catalytic domain structure, which is shallow and shares greatest homology not with other protein phosphatases, but with rhodanese, a highly conserved sulfurtransferase of ambiguous function (14, 15).

We show that bpV compounds have *in vitro* and *in vivo* antineoplastic activity, that they are potent inhibitors of a number of phosphatases, including Cdc25A, and that the specificity and potency of bpV compounds can be effectively modulated by altering the organic heteroligand. This strategy may represent a means for the creation of a novel pharmacophore of antineoplastic agents targeting specific phosphatases pivotal to cancer cell proliferation such as Cdc25A.

## Materials and Methods

### bpV Compounds

bpVs were the generous gift of Dr. Alan Shaver, McGill University. They were synthesized as in Ref. (5) and their structures are shown in Fig. 1. All bpVs were dissolved in PBS and were stored as 100 mM stocks at −20°C and protected from light. Sodium orthovanadate (NaOV) was purchased from Sigma Aldrich Canada, (Oakville, ON, Canada).

### Phosphatase Assays

Glutathione *S*-transferase (GST)-CDC25A was a generous gift of Konstantin Galaktionov. GST-hVH2 (DSP4) was a generous gift of Kun-Liang Guan. *Yersinia pestis* phosphatase (YOPH), T-cell, and leukocyte antigen related/receptor type PTPF catalytic domain (LAR) phosphatases were purchased from Calbiochem-Novabiochem Corp. (San Diego, CA). Phosphatase activity was measured by conversion of *para*-nitrophenol phosphate (PNPP). Assays were performed in a total volume of 105 μl, consisting of 5 μl bpV in PBS, 50 μl 100 mM PNPP, and 50 μl of phosphatase in 2× buffer. $A_{405\ nm}$ was read using a BioTek instruments ELX800 96-well plate reader. Assays proceeded at 37°C. Final buffer concentrations were as follows: *YOPH*: 150 mM NaCl, 100 mM Tris (pH 6.8), 1 mM DTT; *Cdc25A*: 50 mM NaCl, 75 mM Tris (pH 8.0), 1 mM DTT; *DSP4*: 50 mM NaCl, 75 mM Tris (pH 7.5), 1 mM DTT; *LAR, TCPTP*: 50 mM NaCl, 100 mM Tris (pH 7.0), 1 mM DTT.

### Cytotoxicity Assays

All cells were received from American Type Culture Collection, with the exception of HCT116, which was the kind gift of Bert Vogelstein, and SCCA, which was kindly provided by Lawrence Panasci. All cells were grown in RPMI 1640 [10% fetal bovine serum (FBS), 5 CC Pen-Strep], with the exception of LL2 and HCT116, which were grown in DMEM (10% FBS, 5 CC Pen-Strep) and SCCA, which was grown in DMEM low glucose (10% FBS, 5 CC Pen-Strep). Cytotoxicity was assessed by the sulfurhodamine B (SRB) assay, as described in Ref. (16). Briefly, 1000–1500 cells were plated per well in 96-well plates. Twenty-four hours later, inhibitors were added to a final volume of 200 μl. After 96 h, cells were fixed by the addition of 50% ice-cold trichloroacetic acid (TCA) and left at 4°C for 1 h. Plates were then washed 5 times in water, air-dried, and stained for 1 h with 100 μl 0.2% SRB in 1% glacial acetic acid. Excess dye was removed by washing 5 times in 1% glacial acetic acid, then plates were air-dried. SRB was resuspended in 150 μl 10 mM unbuffered Tris (pH 10.5) and $A_{530\ nm}$ was read on a BioTek instruments ELX800 96-well plate reader.

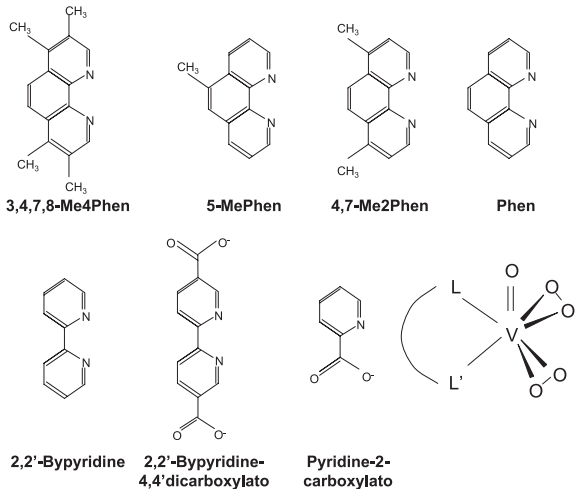


**Figure 1.** Structures of organic heteroligands and core of bpV compounds.

### Apoptosis

SW620 cells were grown to 70% confluence in 10-cm dishes. bpV[1,10-phenanthroline-bisperoxo-oxo-vanadium (Phen)] was added to the medium and cells incubated for a further 48 h. Following incubation with drug, cells were harvested by scraping in the medium and centrifuged. Pelleted cells were washed once in PBS, then lysed with 400 μl lysis buffer [5 mM Tris (pH 7.4), 20 mM EDTA, 0.5% Triton X-100] on ice for 2 h. Membranes and debris were pelleted by centrifugation at 13,000 × *g* for 30 min at 4°C. Thirty-five microliters of RNase A (10 mg/ml stock) were added to the supernatant, which was then incubated at 56°C for 60 min. SDS was added to 1% and Protease K to 0.5 mg/ml, and samples incubated for a further 60 min. Samples were then extracted with 500 μl phenol:chloroform (1:1). DNA was precipitated from the aqueous phase with 100 mM NaCl (final), 1 μl glycogen, and 1 ml 100% ethanol at −20°C. Pellets were washed with 70% ethanol and resuspended in low TE (10 mM Tris:0.1 mM EDTA). Laddering was then assessed by electrophoresis on a 1.8% agarose gel and ethidium bromide (EtBr) staining.

### Western Blotting

Cells were lysed with radioimmunoprecipitation assay (RIPA) buffer in the presence of 1 mM NaOV and proteins electrophoresed on a 10% SDS-PAGE gel. Phospho-specific antibodies (Ser795 and Thr373) were purchased from New England Biolabs, Ltd. (Mississauga, ON, Canada). Anti-phosphotyrosine antibodies were from Upstate Biotechnology Inc. (Lake Placid, NY).

### Fluorescence-Activated Cell Cytometry Analysis

Fluorescence-activated cell sorting (FACS) was performed using standard Propidium Iodide DNA staining methods. Briefly, floating cells were collected and pooled with cells harvested by trypsinization; cells from each treatment condition were then centrifuged at 1000 rpm (160 RCF) in an IEC Centra Cl3R centrifuge, washed once with PBS, and fixed overnight with 70% ethanol in PBS. Fixed cells were then rinsed with PBS, and resuspended in staining solution containing 0.05 mg/ml propidium iodide, 1 mM EDTA, 0.2% Triton X-100, and 0.05 mg/ml RNase A in PBS.

### CDK2 Immunocomplex Kinase Assay

HCT116 cells were plated to 70% confluence, then incubated for 24 h with 0.5, 1.0, or 1.5 μM bpV[4,7-dimethyl-1,10-phenanthroline-bisperoxo-oxo-vanadium (Me2Phen)]. Cells were then rinsed with ice-cold PBS and lysed in 50 mM HEPES (pH 7.4), 50 mM NaCl, 10% glycerol, 0.1% Tween 20, 80 μM β-glycerophosphate, 1 mM phenylmethylsulfonyl fluoride (PMSF), 5 μg/ml aprotinin, and 10 μg/ml leupeptin. Two hundred micrograms of protein were immunoprecipitated overnight using anti-CDK2 antibodies (Santa Cruz Biotechnology, Inc., Santa Cruz, CA; H298) and 20 μl 50% slurry protein G-Sepharose (4 fast-flow, Amersham-Pharmacia Biotech., Baie d'Urfe, QC, Canada). Protein was then washed 3 times with lysis buffer and 3 times with kinase/assay dilution buffer: 20 mM Tris, 0.1 mM NaOV, 1 mM PMSF, 1 mM DTT, 80 μM β-glycerophosphate, 5 μg/ml aprotinin, and 10 μg/ml leupeptin. Ten micrograms/reaction histone H1 (Upstate Biotechnology) was diluted in assay dilution buffer + 10 mM $MgCl_2$ and added to the beads in a volume of 10 μl. Reactions proceeded in a total volume of 50 μl at RT in the presence of 30 μM cold ATP and 5 μCi/reaction [$\gamma$-$^{32}$P]ATP. Reactions were halted after 15 min by addition of 10 μl SDS-PAGE loading dye. Histone H1 was resolved by electrophoresis and visualized by autoradiography. Band intensitywas assessed by SCION image (Scioncorp, Frederick, MD; www.scioncorp.com).

### *In Vivo* Antineoplastic Activity

balb/c mice (Charles River Laboratories, Willmington, MA) were given injections of $0.7 \times 10^6$ DA3 murine mammary carcinoma cells (day 0). Mice bearing palpable tumors at day 4 were randomized. Control mice received normal saline i.p. daily, whereas test mice received 20 mg/kg bpV[Me2Phen] in normal saline i.p. daily for 7 days. Mice were then given a 3-day break from treatment before i.p. injections were resumed every other day. Tumors were measured bidimensionally, and volumes calculated using the formula $(L \times W^2)/2$.

### Statistics

***In Vitro* Cytotoxicity Assays.** $IC_{50}$s represent the mean of experiments containing four replicates for each concentration. $IC_{50}$s were determined in at least two independent experiments.

***In Vivo* Antineoplastic Activity Studies.** Tumors were measured bidimensionally and volumes calculated using the formula $(L \times W^2)/2$. Regression lines were calculated by Graphpad Prism using the formula $Y = Y\text{max}1*(1 - \exp(-K1*X)) + Y\text{max}2*(1 - \exp(-K2*X))$; error bars represent 95% confidence intervals (CIs) of SEs. ANOVA was calculated by a paired, two-tailed $t$ test.

## Results

The panel of bpV compounds shown in Fig. 1 was tested for *in vitro* antineoplastic activity against several cell lines, including SW620 (colon carcinoma), SCC-A (head and neck squamous cell carcinoma), MCF-7 (mammary carcinoma), and Lewis lung (murine lung epithelial cancer); in all tested cell lines, bpV[Me2Phen] was the most potent cytotoxic agent, with submicromolar $IC_{50}$s (data not shown). On the basis of these results, the two most cytotoxic compounds, bpV[Me2Phen] and bpV[Phen], were chosen for further *in vitro* analyses. Twenty-eight cell lines, representing breast, colon, central nervous system (CNS), leukemia, renal, and lung cancers, were subjected to cytotoxicity assays with bpV[Me2Phen] or bpV[Phen] (Table 1).

Of note, there is little or no impact of p53 or p21 status on $IC_{50}$, with matched cell lines HCT116 $p53^{+/+}$ *versus* $p53^{-/-}$ or $p21^{+/+}$ *versus* $p21^{-/-}$ barely differing in their sensitivities to bpV[Me2Phen]. Furthermore, bpV[Phen]-induced apoptosis, as indicated by DNA laddering, was evident after 48 h in p53-mutant SW620 cells (Fig. 2A). We examined global tyrosine phosphorylation following treatment. SW620 cells were treated with bpV[Phen] at concentrations roughly equal to $IC_{50}$ or 10× $IC_{50}$ for 24 h and probed with anti-phosphotyrosine antibodies. Fig. 2B shows that there is a comparable global increase in tyrosine phosphorylation at both concentrations; this may be interpreted as being the result of inhibition of a large number of phosphatases, or of the inhibition or a relatively small number with the concomitant stimulation of signal transduction cascades.

*In vitro* inhibition of phosphatases was then examined using GST fusions of two dual-specificity phosphatases, Cdc25A and the mitogen-activated protein kinase (MAPK) phosphatase hVH2 (DSP4), as well as commercial preparations of three tyrosine phosphatases, YOPH, LAR, and TCPTP. Phosphatase activity was monitored using chromogenic PNPP as a substrate. Fig. 3 shows $IC_{50}$ data for various bpVs (see structures in Fig. 1) and for NaOV. Cdc25A and YOPH were significantly more sensitive to vanadium-based inhibitors than were TCPTP and LAR, with the most potent of the Cdc25A inhibitors being bpV[Phen]. DSP4 was the least sensitive of the phosphatases examined. While this assay does not include enough phosphatases to speak to the specificity of bpVs in the

**Table 1. Cancer cell line $IC_{50}$s on bpV treatment**

| Type | Line | Phen | Me2Phen | Type | Line | Phen | Me2Phen |
|---|---|---|---|---|---|---|---|
| | | $IC_{50}$ (μM) | $IC_{50}$ (μM) | | | $IC_{50}$ (μM) | $IC_{50}$ (μM) |
| Leukemia | Cem | 2.70 | 0.80 | Ovarian | OVCAR3 | 2.00 | 0.84 |
| Leukemia | K562 | 1.25 | 0.30 | Ovarian | OVCAR4 | 2.70 | 0.31 |
| Leukemia | Molt 4 | 1.95 | 0.50 | Renal | 786-0 | 1.12 | 0.63 |
| Leukemia | NB4 | ND | 0.58 | Renal | A498 | 1.05 | 0.75 |
| NSC Lung | A549 | 1.80 | 0.37 | Renal | ACHN | 2.00 | 0.6 |
| NSC Lung | EKVX | 1.40 | 1.05 | Renal | CaKi-1 | 0.45 | 0.34 |
| Lung | LL2 | 1.70 | 0.30 | Renal | UO31 | ND | 0.27 |
| Colon | HCT116 $p21^{+/+}$ | ND | 0.81 | Prostate | PC3 | 2.24 | 0.35 |
| Colon | HCT116 $p21^{-/-}$ | ND | 0.70 | Prostate | DU145 | 1.24 | 0.28 |
| Colon | HCT116 $p53^{+/+}$ | ND | 0.52 | Breast | MCF-7 | 2.95 | 0.84 |
| Colon | HCT116 $p53^{-/-}$ | ND | 0.48 | Breast | NIH ADR | 1.23 | 0.24 |
| Colon | SW620 | 2.61 | 0.78 | Breast | MB 231 | ND | 0.42 |
| CNS | SF295 | ND | 0.49 | Breast | MB 468 | ND | 0.62 |
| CNS | SNB75 | 7.5 | 1.48 | Head and Neck | SCCA | 1.00 | 0.30 |

Note: $IC_{50}$s of cell lines exposed to bpV[Phen] and bpV[Me2Phen]. Cytotoxicity was determined using the SRB assay and a continuous 96-h exposure to bpVs. Micromolar $IC_{50}$s represent the mean of those determined in at least two independent experiments with four replicates per concentration in each experiment.

cellular context (but see Fig. 2B), it does demonstrate that Cdc25A is very sensitive to these compounds, and that organic heteroligand is modulating both potency and specificity.

Next we examined whether Cdc25A is inhibited by bpVs in whole cells. This was done by examining the activity of a direct Cdc25A target, Cdk2, which depends on Cdc25 for activation via removal of inhibitory phosphorylations on T14 and Y15 residues. MCF-7 cells were exposed to bpV[Me2Phen] for 24 h at 0.5, 0.75, and 1.0 μM concentrations. Cells were then harvested and proteins extracted for CDK2 immunoprecipitation. An immunocomplex kinase assay, using histone H1 as a substrate, demonstrated a dose-dependent reduction in CDK2 activity on bpV[Me2-Phen] treatment (Fig. 4A). Similar results were seen in HCT116. Note that MCF-7 exhibited stronger Cdk2 inhibition following bpV treatment than HCT116, despite the fact that the 96-h $IC_{50}$s of the HCT116 cell lines are similar or lower than those observed for MCF-7 (Table 1). This may indicate differing basal levels of Cdc25A or Cdk activity, or a differing propensity of each of these cell lines to induce apoptosis on phosphatase inhibition; these possibilities remain to be investigated. We have also noted that several cell lines with similar 96-h $IC_{50}$s may vary in their rate of cell killing at shorter time points (resulting in differing AUCs); for instance, renal cell lines show signs of significant cell killing by 24 h treatment, whereas other cell lines with similar 96-h $IC_{50}$s show no effects at this time point (data not shown).

The expected downstream result of CDK2 inhibition, hypophosphorylation of Rb, was also examined (Fig. 4B); MCF-7 cells were synchronized by serum starvation then released into serum-containing medium with or without

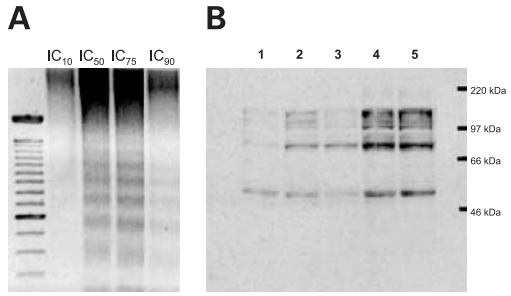


**Figure 2.** **A,** SW620 cells were exposed to bpV[Phen] for 48 h at $IC_{10}$ (1.5 μM), $IC_{50}$ (2.8 μM), $IC_{75}$ (3.6 μM), and $IC_{90}$ (7 μM) before DNA was harvested for agarose gel electrophoresis. **B,** SW620 cells were exposed to bpV[Me2Phen] for 24 h before whole cell extracts were collected and examined for tyrosine phosphorylation by anti-phosphotyrosine Western blot. *Lane 1,* 12 h serum starvation; *lane 2,* 12 h serum starvation followed by 5 min reintroduction of 10% serum; *lane 3,* no treatment; *lane 4,* 24 h exposure to $IC_{50}$ (0.7 μM) bpV[Me2Phen]; *lane 5,* 24 h exposure to 10 × $IC_{50}$ (7.0 μM) bpV[Me2Phen].

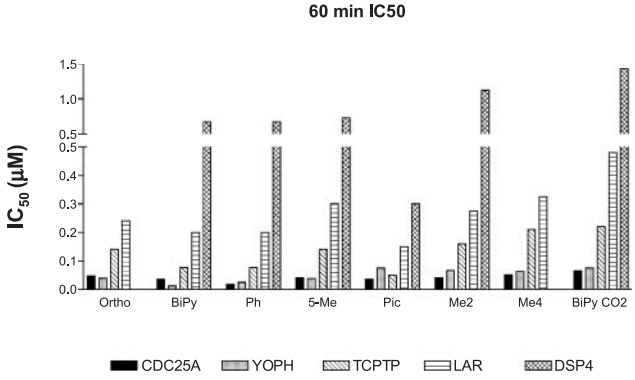


**Figure 3.** $IC_{50}$s of the dual-specificity phosphatases DSP4 and Cdc25A and the PTPs YOPH, LAR, and TCPTP were determined by PNPP conversion and $\Delta A_{405\ nm}$. *BiPy,* 2,2′-bipyridine-bisperoxo-oxovanadium; *5-Me,* 5-methyl-1,10-phenanthroline-bisperoxo-oxo-vanadium; *Pic,* picolinato-bisperoxo-oxo-vanadate; *Me4,* 3,4,7,8-tetramethyl-1,10-phenanthroline-bisperoxo-oxo-vanadium; *BiPy $CO_2$,* 2,2′-bipyridine-4,4′-dicarboxylato-bisperoxo-oxo-vanadate.

1 μM Me2Phen. In the presence of Me2Phen, Rb remained hypophosphorylated despite the presence of serum in the medium. Treatment resulted in $G_1$-S arrest in MCF-7 (Fig. 4C) and all tested cell lines.

Because bpVs contain a reactive metal core with two peroxo groups, they might be expected to produce oxidative stress, which has been proposed as a mechanism of regulation of Cdc25A, because enzyme crystallized in the presence of 3 M NaOV demonstrates disulfide bridge formation between the catalytic cysteine and a conserved cysteine outside the catalytic cleft (15). To address the possibility that this was the mechanism of action of bpVs, we performed cytotoxicity assays after depletion of intracellular glutathione with 50 μM buthionine sulfoximine (BSO) for 24 h. We performed these assays in an Adriamycin-resistant subline of MCF-7, NIH-ADR, which has high glutathione peroxidase activity and a high capacity to inhibit ·OH formation (17). Fig. 5 demonstrates that BSO does not sensitize NIH-ADR cells to bpV[Me2-Phen], although in the positive control for this experiment, this treatment dramatically enhances NaOV cytotoxicity.

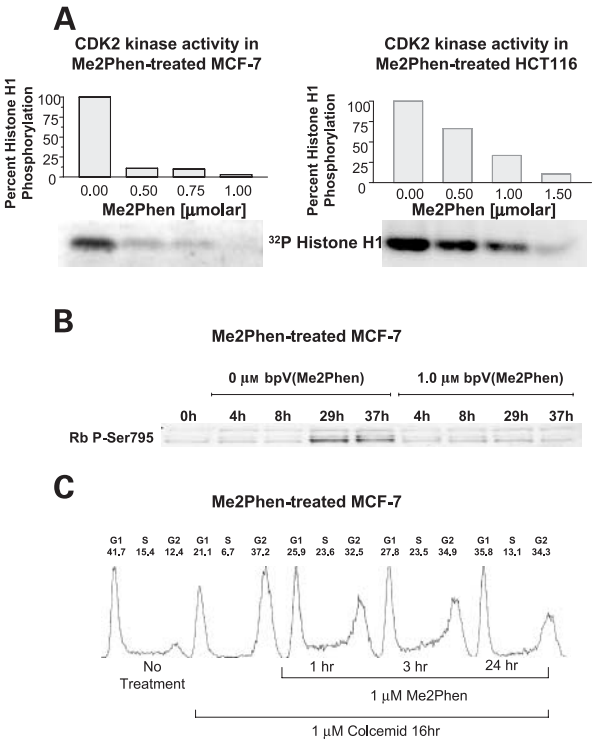


**Figure 4.** **A,** Cdk2 activity in bpV[Me2Phen]-exposed MCF-7 (*left*) and HCT116 (*right*) cells was examined by immunocomplex kinase assay. Cells were exposed to the indicated concentrations of bpV[Me2Phen] for 24 h before Cdk2 was precipitated and assayed for histone H1 kinase activity. **B,** MCF-7 cells were synchronized by serum starvation. Serum-containing medium was then replaced with or without 1 μM Me2Phen. Phosphorylation of Rb was examined in bpV[Me2Phen]-treated MCF-7 using phospho-specific antibodies for pS 795 after 4, 8, 29, or 37 h exposure. Equivalent results were observed using anti-phosphothreonine 373 antibodies (not shown). **C,** cell cycle progression was examined in bpV[Me2Phen]-treated MCF-7. Cells were treated with 1 μM bpV[Me2-Phen] for the indicated times before addition of 1 μM Colcemid overnight. Cells were then analyzed by propidium iodide FACS.

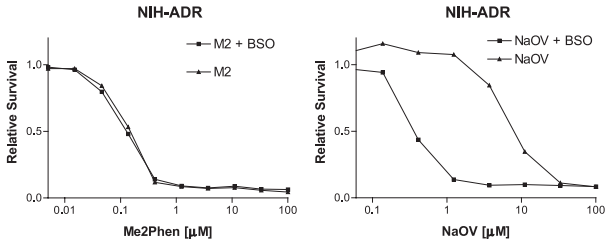


**Figure 5.** Depletion of reduced glutathione (GSH) by incubation of NIH-ADR cells with 50 μM BSO for 24 h sensitizes them to NaOV (*right*) but not to bpV[Me2Phen] (*left*).

Similar results were observed in SW620, where BSO treatment or the presence of exogenous thiol- (glutathione monoethyl ester, PDTC, NAC) or non-thiol- (superoxide dismutase) antioxidants had no effect on bpV[Me2Phen] $IC_{50}$ (not shown).

Another possibility was that bpVs, with their planar heterocycles and polar head groups, were inducing DNA damage. We did not, however, observe any induction of p53 or p21 on bpV treatment (not shown), nor a dependence of $IC_{50}$ on the mutation status of either of these proteins (see Table 1). Furthermore, assays using single cell gel electrophoresis (comet assay) showed no evidence of DNA damage at Me2Phen concentrations as high as 10 μM.[1]

Inhibitors of Cdc25A can be expected to exert their greatest cytotoxic effect on cycling cells, making them candidates for use as antineoplastic agents. To address bpV[Me2Phen]'s *in vivo* efficacy, we used a DA3 mouse mammary carcinoma model in balb/c mice. Mice were given injections of $0.7 \times 10^6$ DA3 cells (day 0), and 20 mg/kg bpV[Me2Phen] i.p. daily beginning when tumors became palpable (day 4). Fifteen mice received bpV[Me2Phen] while 10 controls received saline. After six doses of 20 mg/kg, 6 of 15 mice showed signs of toxicity (mainly dehydration) that were significant enough that they were discontinued from the study. (Given that this dose exceeded what is tolerable, the data presented in Fig. 6 do not include these six animals. However, the inclusion of the data does not substantially affect the curve. The mean tumor size of the Me2Phen-treated group with/without excluded animals ± SE was: day 4 0.087 ± .0079 $cm^3$/0.074 ± 0.01 $cm^3$; day 7 0.098 ± 0.0106 $cm^3$/0.01 ± 0.0148 $cm^3$; day 11 0.097 ± 0.0124 $cm^3$/0.107 ± 0.0194 $cm^3$.) The remaining 9 mice were given a seventh dose, then a 3-day break before injections were resumed on an every-other-day schedule. No mice showed signs of toxicity until day 25 of the study, when one test mouse was found dead; at this point several control mice showed perforation of the skin at the site of the tumor, and the study was terminated. As shown in Fig. 6, bpV[Me2Phen] injection resulted in a sustained inhibition of tumor growth, such that on day 25, tumor volume in test mice was just 20% that of control mice (0.184 $cm^3$ *versus* 0.888 $cm^3$). This difference was significant to $P = 0.0093$ (95% CI difference of means [0.1303 − 0.6109] $cm^3$).

[1] P. J. Scrivens, unpublished data.

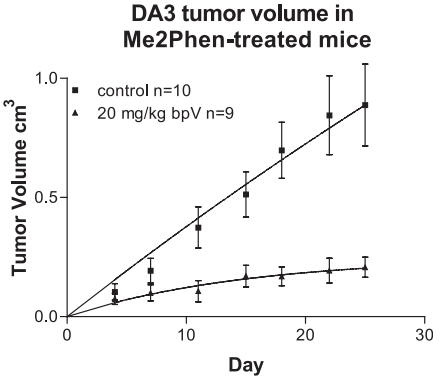


**Figure 6.** Daily i.p. injections of 20 mg/kg bpV[Me2Phen] inhibits tumor growth in DA3-bearing mice. Injections were begun on day 4 when tumors became palpable and continued daily for seven injections. Mice were then given a 3-day break from treatment before injections were resumed; from day 14 to 25, injections were given every second day. At day 25, the experiment was terminated and all mice were sacrificed.

## Discussion

The potential of phosphatase inhibitors as antineoplastic agents has remained somewhat overlooked, perhaps because the role of protein phosphatases is seen as largely homeostatic, in that they function to return activated receptors and other kinases to the ground state. While this may indeed be the role of many phosphatases, it belies the importance of this large family of enzymes in controlling major facets of cellular growth and proliferation. Perceptually, inhibition of protein phosphatases could be antineoplastic via a myriad of mechanisms. Generalized dysregulation of growth factor pathways might itself trigger apoptosis. Alternatively, dysregulation of protein phosphorylation may have a direct impact on apoptotic pathways, or on homeostatic pathways such as translation. Yet another possibility is that cell death could be induced by inhibition of an activating phosphatase which is required for cellular proliferation. Such an example is Cdc25A and its related family members.

We examined the ability of a panel of stable bpV species to inhibit cellular proliferation *in vitro* and *in vivo*. We found that the *in vitro* efficacy of the compounds as antineoplastic agents against a panel of cancer cell lines varied greatly with modification of the organic heteroligand coordinating the metal core. The most potent of the compounds *in vitro* had submicromolar $IC_{50}$s in most cell lines tested, and showed some promise *in vivo*, halting the growth of tumors in a DA3 murine mammary tumor model. While these species contain a reactive heavy metal core coordinated by a planar heterocycle and two peroxo groups, our evidence suggests that neither DNA damage nor oxidative stress plays a role in the observed cytotoxicity. In contrast, phosphatase inhibition, as evidenced by a global increase in tyrosine phosphorylation, was evident in whole cells at $IC_{50}$ concentrations.

The bpV compounds were assayed for their ability to inhibit a panel of phosphatases *in vitro*. These assays demonstrated that a wide variety of PTPs could be inhibited by bpV compounds with $IC_{50}$s in the nanomolar range. Cdc25A and YOPH were the two most sensitive phosphatases tested. Furthermore, this study demonstrates that both the specificity and the potency of the bpV compounds can be modulated by modification of the organic heterocycle. The inhibition of Cdc25A in whole cells was demonstrated by the effects on downstream signals including: cell cycle arrest, Rb hypophosphorylation, and Cdk2 inactivation on treatment with $IC_{50}$ doses of bpVs. These effects do not appear to be modulated by induction of p53 or p21. The latter result appears to contrast with a published report suggesting that Cdc25A may directly interact with the Cut homeodomain protein, activating the latter as a repressor of p21 expression (18). In that study, Cdc25A was examined for Cut interaction because of its role in $G_1$-S progression, corresponding to Cut activation in synchronized/released cells. Although it is difficult to reconcile these observations without further studies, it is clear that Cdc25A is not solely responsible for Cut regulation, as both phosphorylation-dephosphorylation of Cut and its protein levels contribute to its activity. Furthermore, Cdc25A was examined as a potential Cut phosphatase because of its role in $G_1$-S (a role that is now being reevaluated, see below); there has not, however, been an extensive survey of cell cycle-dependent phosphatase expression/activity. Thus, it remains possible that another phosphatase may function similarly to Cdc25A with respect to Cut regulation.

Cdc25A is overexpressed in several cancers and is presumed to be essential for cellular proliferation, given its central position both in the normal cell cycle and as a target of several checkpoint pathways. Cdc25 family members are required for activation of Cdks via removal of inhibitory phosphorylations. Activation of the Cdks in $G_1$ leads to cell cycle progression through S phase via Rb hyperphosphorylation and, in the case of Cdc25A, enhanced activity as a result of a positive feedback loop with Cdk2 (19). Following replication of the chromosomes, the cell division cycle culminates with the Cdc25-dependent activation of Cdc2/Cdk1, resulting in the major structural rearrangements observed in M phase.

The Cdc25A catalytic domain has been crystallized, and is characterized by a shallow topology which is distinct from that of other known protein phosphatases, including other dual-specificity phosphatases (14, 15). In fact, the domain is structurally most similar to rhodanese, a conserved sulfurtransferase, the precise role of which remains ambiguous. The shallow catalytic cleft enhances the attractiveness of Cdc25A as a target, as it may allow the use of relatively large inhibitors sterically excluded from the catalytic domains of other phosphatases.

The three human isoforms of Cdc25 (*i.e.*, Cdc25A, -B, and -C) demonstrate considerable homology within their catalytic domains. Thus, it is certainly possible that the other two isoforms (Cdc25B and -C) may be inhibited by bpVs, although this was not tested in this study. It is notable, however, that treatment of cells with bpVs resulted in $G_1$-S arrest under the conditions we used. This is particularly interesting in light of recent studies indicating a role for

Cdc25A in M phase (20, 21). According to these studies, Cdc25A is a bi-stable enzyme, reaching maximal stability in M phase as a result of cyclin-cdk phosphorylation. Moreover, recent studies indicate that cyclin-cdk phosphorylation of Cdc25s renders them insensitive to certain checkpoint stimuli in a cell cycle phase-dependent manner (22, 23). These studies seem to indicate that the traverse of M phase is dependent on a crescendo of Cdc25 (and therefore cyclin-cdk) activity commencing in $G_1$. This process begins with Cdc25A in $G_1$ and is followed by an increase in Cdc25B and -C in S and $G_2$, respectively. It appears that all three may act in concert to affect progression through mitosis. While all three Cdc25s may play a role in the latter stages of the cell cycle, it is difficult to predict the effect of the inhibition of individual isoforms on cell cycle progression. In an early paper reporting activation of Cdc25A by cyclin B alone, inactivating antibodies were microinjected into cells and resulted in M-phase arrest (24). In contrast, a number of subsequent studies established a role for Cdc25A much earlier in the cell cycle (25), and, notably, demonstrated a $G_1$-S blockade on antibody microinjection (26). Furthermore, knockout of Cdc25C resulted in no apparent cell cycle perturbation (27). Thus, the fact that bpVs do not arrest cells in M phase despite the recently demonstrated role for Cdc25A in this phase is consistent with previous observations and with our knowledge of the cell cycle expression and activity of these enzymes.

In this study, we have demonstrated that bpV compounds are potent antineoplastic agents. Their antineoplastic activity is associated with phosphatase inhibition in whole cells and does not appear to result from DNA damage or oxidative stress. The bpVs inhibit several phosphatases *in vitro*, including Cdc25A; their specificity and potency being modulated by their organic heterocycles. We therefore conclude that bpV compounds represent lead compounds which can be readily modified to enhance their specificity toward a variety of cellular phosphatase targets. Cdc25A represents a promising target which is strongly inhibited by bpV compounds *in vitro* and in whole cells.

### References


**1.** Simons, T. J. Vanadate—a new tool for biologists. Nature, *281:* 337–338, 1979.

**2.** Cruz, T. F., Morgan, A., and Min, W. *In vitro* and *in vivo* antineoplastic effects of orthovanadate. Mol. Cell. Biochem., *153:* 161–166, 1995.

**3.** Djordjevic, C. Antitumor activity of vanadium compounds. Met. Ions Biol. Syst., *31:* 595–616, 1995.

**4.** Shaver, A., Ng, J. B., Hall, D. A., and Posner, B. I. The chemistry of peroxovanadium compounds relevant to insulin mimesis. Mol. Cell. Biochem., *153:* 5–15, 1995.

**5.** Posner, B. I., Faure, R., Burgess, J. W., Bevan, A. P., Lachance, D., Zhang-Sun, G., Fantus, I. G., Ng, J. B., Hall, D. A., Lum, B. S., and Shaver, A. Peroxovanadium compounds. A new class of potent phosphotyrosine phosphatase inhibitors which are insulin mimetics. J. Biol. Chem., *269:* 4596–4604, 1994.

**6.** Foot, E. A., Bliss, T., Da Costa, C., and Leighton, B. Dose related stimulation of glucose metabolism by peroxovanadate in rat skeletal muscle preparations *in vitro*. Biochem. Soc. Trans., *19:* 133S, 1991.

**7.** Bevan, A. P., Drake, P. G., Yale, J. F., Shaver, A., and Posner, B. I. Peroxovanadium compounds: biological actions and mechanism of insulin-mimesis. Mol. Cell. Biochem., *153:* 49–58, 1995.

**8.** Gasparotto, D., Maestro, R., Piccinin, S., Vukosavljevic, T., Barzan, L., Sulfaro, S., and Boiocchi, M. Overexpression of CDC25A and CDC25B in head and neck cancers. Cancer Res., *57:* 2366–2368, 1997.

**9.** Cangi, M. G., Cukor, B., Soung, P., Signoretti, S., Moreira, G., Jr., Ranashinge, M., Cady, B., Pagano, M., and Loda, M. Role of the Cdc25A phosphatase in human breast cancer. J. Clin. Invest., *106:* 753–761, 2000.

**10.** Galaktionov, K., Lee, A. K., Eckstein, J., Draetta, G., Meckler, J., Loda, M., and Beach, D. CDC25 phosphatases as potential human oncogenes. Science, *269:* 1575–1577, 1995.

**11.** Mailand, N., Falck, J., Lukas, C., Syljuasen, R. G., Welcker, M., Bartek, J., and Lukas, J. Rapid destruction of human Cdc25A in response to DNA damage. Science, *288:* 1425–1429, 2000.

**12.** Falck, J., Mailand, N., Syljuasen, R. G., Bartek, J., and Lukas, J. The ATM-Chk2-Cdc25A checkpoint pathway guards against radioresistant DNA synthesis. Nature, *410:* 842–847, 2001.

**13.** Bulavin, D. V., Higashimoto, Y., Popoff, I. J., Gaarde, W. A., Basrur, V., Potapova, O., Appella, E., and Fornace, A. J., Jr. Initiation of a G2/M checkpoint after ultraviolet radiation requires p38 kinase. Nature, *411:* 102–107, 2001.

**14.** Hofmann, K., Bucher, P., and Kajava, A. V. A model of Cdc25 phosphatase catalytic domain and Cdk-interaction surface based on the presence of a rhodanese homology domain. J. Mol. Biol., *282:* 195–208, 1998.

**15.** Fauman, E. B., Cogswell, J. P., Lovejoy, B., Rocque, W. J., Holmes, W., Montana, V. G., Piwnica-Worms, H., Rink, M. J., and Saper, M. A. Crystal structure of the catalytic domain of the human cell cycle control phosphatase, Cdc25A. Cell, *93:* 617–625, 1998.

**16.** Skehan, P., Storeng, R., Scudiero, D., Monks, A., McMahon, J., Vistica, D., Warren, J. T., Bokesch, H., Kenney, S., and Boyd, M. R. New colorimetric cytotoxicity assay for anticancer-drug screening. J. Natl. Cancer Inst., *82:* 1107–1112, 1990.

**17.** Batist, G., Tulpule, A., Sinha, B. K., Katki, A. G., Myers, C. E., and Cowan, K. H. Overexpression of a novel anionic glutathione transferase in multidrug-resistant human breast cancer cells. J. Biol. Chem., *261:* 15544–15549, 1986.

**18.** Coqueret, O., Berube, G., and Nepveu, A. The mammalian Cut homeodomain protein functions as a cell-cycle-dependent transcriptional repressor which downmodulates p21WAF1/CIP1/SDI1 in S phase. EMBO J., *17:* 4680–4694, 1998.

**19.** Hoffmann, I., Draetta, G., and Karsenti, E. Activation of the phosphatase activity of human cdc25A by a cdk2-cyclin E dependent phosphorylation at the G1/S transition. EMBO J., *13:* 4302–4310, 1994.

**20.** Donzelli, M., Squatrito, M., Ganoth, D., Hershko, A., Pagano, M., and Draetta, G. F. Dual mode of degradation of Cdc25 A phosphatase. EMBO J., *21:* 4875–4884, 2002.

**21.** Mailand, N., Podtelejnikov, A. V., Groth, A., Mann, M., Bartek, J., and Lukas, J. Regulation of G(2)/M events by Cdc25A through phosphorylation-dependent modulation of its stability. EMBO J., *21:* 5911–5920, 2002.

**22.** Bulavin, D. V., Higashimoto, Y., Demidenko, Z. N., Meek, S., Graves, P., Phillips, C., Zhao, H., Moody, S. A., Appella, E., Piwnica-Worms, H., and Fornace, A. J. Dual phosphorylation controls Cdc25 phosphatases and mitotic entry. Nat. Cell Biol., *5:* 545–551, 2003.

**23.** Bulavin, D. V., Demidenko, Z. N., Phillips, C., Moody, S. A., and Fornace, A. J., Jr. Phosphorylation of *Xenopus* Cdc25C at Ser285 interferes with ability to activate a DNA damage replication checkpoint in pre-midblastula embryos. Cell Cycle, *2:* 263–266, 2003.

**24.** Galaktionov, K. and Beach, D. Specific activation of cdc25 tyrosine phosphatases by B-type cyclins: evidence for multiple roles of mitotic cyclins. Cell, *67:* 1181–1194, 1991.

**25.** Blomberg, I. and Hoffmann, I. Ectopic expression of Cdc25A accelerates the G(1)/S transition and leads to premature activation of cyclin E- and cyclin A-dependent kinases. Mol. Cell. Biol., *19:* 6183–6194, 1999.

**26.** Jinno, S., Suto, K., Nagata, A., Igarashi, M., Kanaoka, Y., Nojima, H., and Okayama, H. Cdc25A is a novel phosphatase functioning early in the cell cycle. EMBO J., *13:* 1549–1556, 1994.

**27.** Chen, M. S., Hurov, J., White, L. S., Woodford-Thomas, T., and Piwnica-Worms, H. Absence of apparent phenotype in mice lacking Cdc25C protein phosphatase. Mol. Cell. Biol., *21:* 3853–3861, 2001.